7048 *Macromolecules* **2010**, *43*, 7048–7055
DOI: 10.1021/ma1011655

Macromolecules
ARTICLE

New Dual Initiators To Combine Quasiliving Carbocationic Polymerization and Atom Transfer Radical Polymerization

Yaling Zhu and Robson F. Storey*

School of Polymers and High Performance Materials, The University of Southern Mississippi, 118 College Drive # 5050, Hattiesburg, Mississippi 39406

Received May 25, 2010; Revised Manuscript Received June 19, 2010

ABSTRACT: New dual initiators, 3,3,5-trimethyl-5-chlorohexyl 2-bromopropionate (IB_2BP) and 3,3,5-trimethyl-5-chlorohexyl 2-bromo-2-methylpropionate (IB_2BMP), which contain initiating sites for both carbocationic polymerization and atom transfer radical polymerization (ATRP), were synthesized and used to create poly(isobutylene-*b*-methyl acrylate) (PIB-*b*-PMA) diblock copolymers. Initiator synthesis involved reaction of methyl 3,3-dimethyl-4-pentenoate with 2 equiv of methylmagnesium bromide, followed by hydroboration−oxidation of the double bond to yield 1,5-dihydroxy-3,3,5-trimethylhexane (DHTMH). IB_2BP was synthesized by reaction of the primary hydroxyl group of DHTMH with 2-bromopropionyl bromide, followed by chlorination of the tertiary hydroxyl group with anhydrous HCl. IB_2BMP was synthesized analogously using 2-bromo-2-methylpropionyl bromide. Both initiators displayed slow cationic initiation of isobutylene, leading to moderate initiation efficiencies ($0.50 < I_{eff} < 0.80$) at low temperature (−70 °C) and low monomer/initiator ratio (82). Higher cationic initiation efficiency ($0.80 < I_{eff} < 0.90$) was observed when temperature was increased to −50 °C and/or the monomer/initiator ratio was increased. In spite of low I_{eff}, the resulting PIBs had narrow polydispersity, and each chain contained one intact 2-bromopropionyl head group, which was subsequently used for ATRP of methyl acrylate. Efficiency of radical initiation was very high, and targeted PMA block lengths were obtained.

Introduction

Block copolymers have received considerable attention due to their unique physical properties, which are related to their ability to self-assemble into ordered morphologies. Block copolymers containing elastomeric segments based on polyisobutylene (PIB) are of great interest because of the exceptional oxidative and chemical resistance, superior gas barrier and mechanical damping characteristics, and excellent biocompatibility of PIB. In the early 1990s, Kennedy and co-workers were the first to synthesize PS−PIB−PS block copolymers via quasiliving carbocationic polymerization (QCP) and the technique of sequential monomer addition, involving bidirectional polymerization of isobutylene (IB) followed by addition of styrene (S).[1,2] These triblock copolymers possessed discontinuous PS glassy domains, which provided thermally reversible, physical cross-linking and a continuous PIB rubbery phase, which imparted material flexibility. Over the years other cationically polymerizable monomers including α-methylstyrene,[3−5] *p*-methylstyrene,[6,7] *p*-chlorostyrene,[8] and methyl vinyl ether[9] have also been combined with PIB using the technique of sequential monomer addition. However, for cases where the second monomer is significantly more reactive than isobutylene, good blocking efficiency has required additional steps, developed principally by Faust et al.,[5] whereby a nonhomopolymerizable olefin such as 1,1-diphenylethylene is first added to quasiliving PIB to affect complete ionization of the chain ends, followed by adjustment of the Lewis acidity and introduction of the second monomer.

Although the technique of sequential monomer addition is simple and direct, it is limited to those monomer combinations that are polymerizable by the same mechanism: anionic, cationic, radical, etc. To create block copolymers from monomers that cannot be polymerized by the same mechanism, one may couple existing prepolymers or combine different controlled/living polymerization methods using either site (mechanism) transformation or a dual initiator approach. Site transformation has been employed to convert the growing chain ends of a cationically derived polymer into an initiating site for several different types of polymerization processes including atom transfer radical polymerization (ATRP),[10−15] reversible addition−fragmentation chain transfer (RAFT) polymerization,[16,17] anionic olefin polymerization,[18−20] and anionic ring-opening polymerization.[21,22] Dual initiators contain initiating sites for two different polymerization processes within the same molecule. Only a few dual initiators have been reported in which one site is a cationic polymerization initiator. Du Prez et al. reported the compound 3,3-diethoxypropyl 2-bromo-2-methylpropionate, which contains an acetal function for initiation of cationic polymerization of a vinyl ether monomer and a 2-bromo-2-methylpropionate function for initiation of ATRP of an acrylate or methacrylate monomer.[23] Du Prez et al.[24,25] also reported the compound 4-hydroxybutyl 2-bromo-2-methylpropionate, which contains the same ATRP initiating site and whose primary hydroxyl group serves as an initiator for cationic ring-opening polymerization of THF, after activation with triflic anhydride. Schubert et al.[26] used 2-bromo-2-methylpropionyl bromide for the cationic ring-opening polymerization of 2-ethyl-2-oxazoline and subsequent ATRP initiation of styrene.

Of particular relevance to this work, Storey et al.[27] reported synthesis of the latent dual initiator, 3,3,5-trimethyl-5-chlorohexyl acetate (TMCHA), a carbocationic initiator containing a blocked hydroxyl group, which was subsequently converted to an ATRP initiator. TMCHA was first used as a cationic initiator to create PIB−PS block copolymers, and it was demonstrated that the

*To whom correspondence should be addressed.

 Published on Web 08/04/2010

Scheme 1. Synthesis of 3,3,5-Trimethyl-5-chlorohexyl 2-Bromopropionate (IB_2BP) and 3,3,5-Trimethyl-5-chlorohexyl 2-Bromo-2-methylpropionate (IB_2BMP)

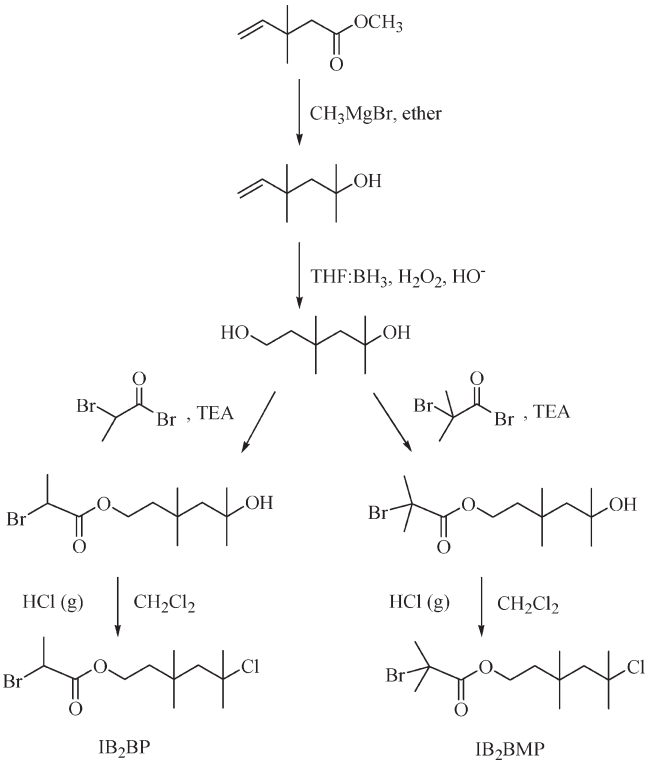

primary acetoxy group remains intact throughout the carbocationic polymerization process. After cationic polymerization, the acetate group was easily converted back to a primary hydroxyl group, and the latter was converted to an ATRP initiator by reaction with 2-bromopropionyl bromide. The resulting macroinitiator was used to produce poly(*tert*-butyl acrylate) under ATRP conditions, which was then hydrolyzed to form poly(acrylic acid) (PAA)−PIB−PS triblock copolymers. Disadvantages of TMCHA were its low initiation efficiency (I_{eff}) during cationic polymerization and the tedious, two-step site transformation reaction prior to ATRP. Although the authors did not fully understand the cause for low I_{eff}, it was interpreted to be related to the complexation of the ester carbonyl group with the Lewis acid $TiCl_4$.

In this paper, we have developed two new dual initiators, 3,3,5-trimethyl-5-chlorohexyl 2-bromopropionate (IB_2BP) and 3,3,5-trimethyl-5-chlorohexyl 2-bromo-2-methylpropionate (IB_2BMP). These compounds have a cationic initiating site identical to that of TMCHA, but the acyl groups contain a bromine atom bonded to the α carbon and are thus ATRP-ready. The bromide function was predicted to be very difficultly ionized, even by the strong Lewis acids used in carbocationic polymerization since ionization would place a positive charge on a carbon that is α to a carbonyl group, which would be extremely unstable. The bulkiness and electron-withdrawing nature of bromine were also predicted to diminish the tendency toward interaction of the carbonyl oxygen with Lewis acids, thus potentially improving I_{eff}. Comparing the two compounds, the 2-bromo-2-methylpropionate group of IB_2BMP would be less resistant toward ionization, but it would be more bulky, providing more steric suppression of complexation. The synthesis of these two initiators is outlined in Scheme 1. We have demonstrated their utility by synthesizing PIB-*b*-PMA diblock copolymers. Methyl acrylate (MA) was chosen as a model ATRP monomer since its methoxyl group provides a well-separated, easily quantifiable signal in ^1H NMR.

Scheme 2. Synthesis of PIB-*b*-PMA Copolymers

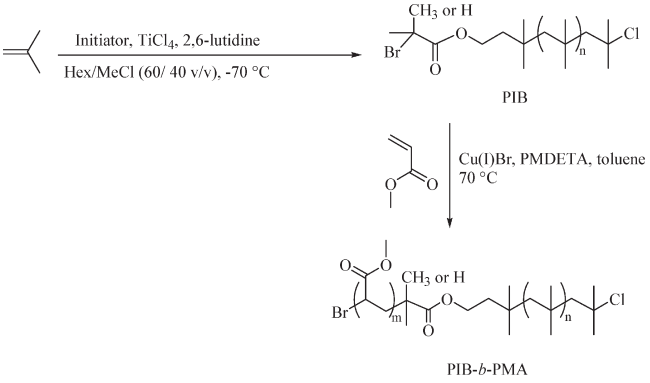

The general synthesis of the PIB-*b*-PMA diblock copolymer is illustrated in Scheme 2. It involves first the QCP of IB from the *tert*-chloride function of the initiator, followed by ATRP of MA from the resulting macroinitiaor yielding PIB-*b*-PMA diblock copolymer. The synthesis can be easily extended to form ABC triblock copolymers such as PS-*b*-PIB-*b*-PMA.

Experimental Section

Materials. Methyl 3,3-dimethyl-4-pentenoate was used as received from TCI America. Methylmagnesium bromide (3 M solution in diethyl ether), borane−tetrahydrofuran (THF) complex (1 M solution in THF), hydrogen peroxide (30 wt % solution in water), 2-bromopropionyl bromide (97%), 2-bromo-2-methylpropionyl bromide (98%), triethylamine (99.5%), silica gel (70−230 mesh, 60 Å, for column chromatography), hexane (anhydrous, 99%), 2,6-lutidine (99+%), $TiCl_4$ (99.9%, packaged under N_2 in Sure-Seal bottles), Cu(I)Br (99.999%), aluminum oxide (activated, neutral, Brockmann I, ~150 mesh, 58 Å), 1,1,4,7,7-pentamethyldiethylenetriamine (PMDETA), toluene (anhydrous, 99.8%), and deuterated chloroform were used as received from Sigma-Aldrich, Inc. Diethyl ether (spectranalyzed), methylene chloride (99.9%), tetrahydrofuran (HPLC grade), heptane (HPLC grade), sodium chloride, potassium carbonate, sulfuric acid, magnesium sulfate, calcium chloride, sodium bicarbonate, and sodium hydroxide were used as received from Fisher Chemical Co. Isobutylene (IB) (99.5%, BOC Gases) and CH_3Cl (MeCl) (99.5%, Alexander Chemical Co.) were dried through columns packed with $CaSO_4$ and $CaSO_4$/4 Å molecular sieves, respectively. Methyl acrylate (MA) (99%, Sigma-Aldrich) was passed through a potassium carbonate and aluminum oxide column to remove inhibitor.

Instrumentation. Molecular weights and polydispersity index (PDI) of polymers were determined using a GPC system consisting of a Waters Alliance 2695 separations module fitted with online multiangle laser light scattering (MALLS) detector (MiniDAWN, Wyatt Technology, Inc.), interferometric refractometer (Optilab rEX, Wyatt Technology Inc.), and online differential viscometer (ViscoStar, Wyatt Technology, Inc.), all operating at 35 °C, and either two mixed E (3 μm bead size) or two mixed D (5 μm bead size) PL gel (Polymer Laboratories Inc.) GPC columns connected in series. Freshly distilled THF served as the mobile phase and was delivered at a flow rate of 1.0 mL/min. Samples were prepared by dissolving 10−12 mg polymer into 1.5 g of freshly distilled THF, and the injection volume was 100 μL. The detector signals were recorded using ASTRA software (Wyatt Technology Inc.), and PIB homopolymer molecular weights were determined using an assumed dn/dc given by the following equation:[28] dn/dc = 0.116(1 − 108/$\bar{M}_n$) ($\bar{M}_n$ = number-average molecular weight). PIB-*b*-PMA block polymers were analyzed using a dn/dc calculated from the refractive index detector response and assuming 100% mass recovery from the columns.

Solution ^{1}H NMR spectra were obtained on a Varian Mercury^{plus} NMR spectrometer operating at a frequency of 300.13 MHz, using 5 mm o.d. tubes with sample concentrations of 5−7% (w/v) in deuterated chloroform ($CDCl_3$) (Aldrich Chemical Co.) containing tetramethylsilane (TMS) as an internal reference. All shifts were referenced automatically by the software (VNMR 6.1C) using the resonance frequency of TMS (0 ppm).

A ReactIR 4000 reaction analysis system (light conduit type), equipped with a DiComp (diamond composite) insertion probe, a general-purpose platinum resistance thermometer, and CN76000 series temperature controller (Omega Engineering, Stamford, CT), was used to collect spectra of the polymerization components and monitor reaction temperature in real time. The light conduit and probe were contained within a drybox (MBraun Labmaster 130) equipped with a thermostated hexane/heptane cold bath.

Procedures. *Initiator Synthesis*. The overall synthesis of IB_2BP and IB_2BMP is illustrated in Scheme 1. The Grignard and hydroboration−oxidation reactions were carried out as previously described.[27] Esterification of 1,5-dihydroxy-3,3,5-trimethylhexane was performed using 2-bromopropionyl bromide or 2-bromo-2-methylpropionyl bromide. After applying column chromatography to remove impurities, dry, gaseous HCl was bubbled through a solution of the purified ester in CH_2Cl_2 to chlorinate the tertiary hydroxyl group.

Esterification. To a 500 mL three-neck, round-bottom flask, equipped with magnetic stirrer, and nitrogen inlet/outlet, were charged triethylamine (2.2 mL, 0.016 mol) and 1,5-dihydroxy-3,3,5-trimethylhexane (2.5 g, 0.016 mol) dissolved in 20 mL of THF. 2-Bromopropionyl bromide (3.9 g, 0.018 mol) dissolved in 10 mL of THF was added dropwise via syringe, and a light-orange precipitate appeared. The reaction was allowed to proceed for 5 h. Then 100 mL of diethyl ether was added to the flask, and the mixture was washed thrice with deionized water (DI H_2O) and dried over magnesium sulfate. After removing the solvent, the crude product, 5-hydroxy-3,3,5-trimethylhexyl 2-bromopropionate, was obtained as a yellow liquid in 89% yield (4.1 g).

5-Hydroxy-3,3,5-trimethylhexyl 2-bromo-2-methylpropionate was synthesized similarly using 2-bromo-2-methylpropionyl bromide (crude yield 95%).

Column Chromatography. Before chlorination, crude 5-hydroxy-3,3,5-trimethylhexyl 2-bromopropionate (4.1 g) was passed through a 15 cm silica gel column, using 9/1 (v/v) heptane/THF (9/1, v/v) cosolvents as the eluent. A clear, yellow liquid was obtained in 53% yield (2.4 g). 5-Hydroxy-3,3,5-trimethylhexyl 2-bromo-2-methylpropionate was treated similarly and obtained as a colorless liquid in 47% yield.

Chlorination. Dry, gaseous HCl, formed by dripping sulfuric acid over sodium chloride, was bubbled through a solution of 5-hydroxy-3,3,5-trimethylhexyl 2-bromopropionate (2.4 g, 8.1×10^{-3} mol) in 30 mL of methylene chloride for 5 h. The liquid product, IB_2BP, was obtained in 91% yield (2.8 g). IB_2BMP was obtained in the same way.

PIB Synthesis. The following procedure was employed for polymerizations of IB initiated by IB_2BP or IB_2BMP within an inert atmosphere drybox equipped with a hexane/heptane cold bath. FTIR (ReactIR 4000) was used to monitor isobutylene conversion by observing the olefinic $=CH_2$ wag (887 cm^{-1}) of IB.[29] The DiComp probe was inserted into a 250 mL four-necked round-bottom flask equipped with a temperature probe and a stirring shaft with a Teflon paddle. The reactor was placed into the cold bath and allowed to equilibrate to −70 °C. Into the flask were charged 57.9 mL of prechilled hexane, 38.6 mL of prechilled MeCl, 2,6-lutidine (0.0489 mL, 4.23×10^{-4} mol), and IB_2BMP (0.4224 g, 1.29×10^{-3} mol). The mixture was allowed to stir for 10 min to reach thermal equilibrium, after which a background spectrum was collected. Prechilled IB (8.50 mL, 0.106 mol) was added to the flask, and then about 15 spectra were obtained to establish the average intensity at 887 cm^{-1}, A_0, corresponding to the initial monomer concentration. Then $TiCl_4$ (0.565 mL, 5.16×10^{-3} mol) was injected into the flask. The molar concentrations of reagents were $[IB]_0 = 1.00$ M, $[I]_0 = 12.2$ mM, $[2,6\text{-lutidine}]_0 = 4.00$ mM, and $[TiCl_4]_0 = 48.8$ mM. Once the monomer was fully consumed, which was indicated by the 887 cm^{-1} absorbance approaching an asymptotic value, A_r, 20 mL of prechilled CH_3OH was added to quench the polymerization. After warming to room temperature and loss of MeCl, the hexane layer was washed with CH_3OH and DI H_2O and dried over magnesium sulfate. PIB samples were then precipitated from MeOH and dried under vacuum to yield a colorless viscous liquid.

Monomer concentration at a given reaction time, $[M]_t$, was calculated from the intensity of the 887 cm^{-1} absorbance at that time, A_t, using the following equation, where $[M]_0$ is the original monomer concentration:

$$[M]_t = [M]_0 \frac{A_t - A_r}{A_0 - A_r} \quad (1)$$

PIB-b-PMA Synthesis. ATRP of MA was performed using Cu(I)Br as a catalyst, PMDETA as a ligand, and PIB with 2-bromo-2-methylpropionate (BMP-PIB) or 2-bromopropionate head group (BP-PIB) as the macroinitiator (MacroI).[27,30] Polymerizations were performed with molar ratio $[MacroI]_0$:$[CuBr]_0$:$[PMDETA]_0$ = 1:1:1 in toluene with $[MacroI]_0 = 0.05$ M, at 70 °C, targeting $\bar{X}_n$ of 60, 90, or 120. The number-average molecular weight for the BP-PIB via GPC was 5570 g/mol; the PDI was 1.04, and $\bar{X}_n = 89$ by NMR. The number-average molecular weight for the BMP-PIB via GPC was 4650 g/mol; the PDI was 1.02, and $\bar{X}_n = 77$ by NMR.

The following procedure was employed for ATRP of MA. A dry Schlenk flask was charged with BMP-PIB (0.93 g, 1.7×10^{-4} mol), MA (1.8 mL, 2.0×10^{-2} mol), CuBr (0.029 g, 2.0×10^{-4} mol), and 4 mL of anhydrous toluene. After three freeze−pump−thaw cycles, PMDETA (0.042 mL, 2.0×10^{-4} mol) was added to the reaction mixture via a deoxygenated syringe. Then the reaction mixture was immersed in an oil bath at 70 °C. Aliquots were taken every half hour, and the progress of polymerization was monitored by observing diminution of the olefinic resonances of monomer in the ^{1}H NMR spectrum. The polymerization was allowed to proceed for several hours to reach a monomer conversion of about 60%. After polymerization, the polymer solution was passed through an aluminum oxide-packed column to remove the copper salt. Then 15−20 mL of THF was added to completely dissolve the polymer, and the resulting solution was passed through a filter with pore size 0.2 μm to remove Al_2O_3. PIB-*b*-PMA samples were then precipitated into MeOH and dried under vacuum to yield a solid product.

Results and Discussion

Initiator Synthesis. New initiators, IB_2BP and IB_2BMP, for QCP of IB were synthesized via the route shown in Scheme 1. Synthesis of the common intermediate, 1,5-dihydroxy-3,3,5-trimethylhexane, has been reported.[27] Esterification to attach either the 2-bromopropionoyl or the 2-bromo-2methylpropionoyl moiety was carried out in each case using the acid bromide in THF solution with triethylamine as acid scavenger. Upon esterification with either acid bromide, the products were contaminated by impurities, which could not be simply eliminated by extraction. However, by passing either crude product through a silica gel column and eluting with heptane/THF (9/1, v/v) cosolvents, pure product was obtained in ∼50% yield.

Figure 1 shows ^{1}H NMR spectra of 5-hydroxy-3,3,5-trimethylhexyl 2-bromopropionate (upper) and 5-hydroxy-3,3,5-trimethylhexyl 2-bromo-2-methylpropionate (lower) after column chromatography. For both compounds, the methylene protons formerly next to the primary hydroxyl

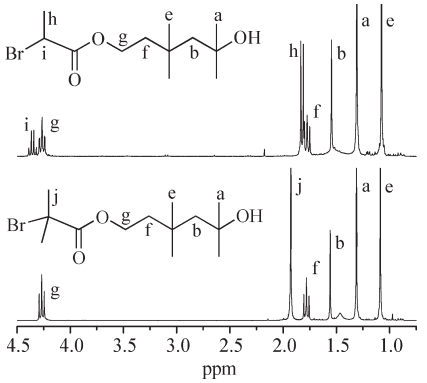

Figure 1. ^{1}H NMR spectra of 5-hydroxy-3,3,5-trimethylhexyl 2-bromopropionate (upper) and 5-hydroxy-3,3,5-trimethylhexyl 2-bromo-2-methylpropionate (lower).

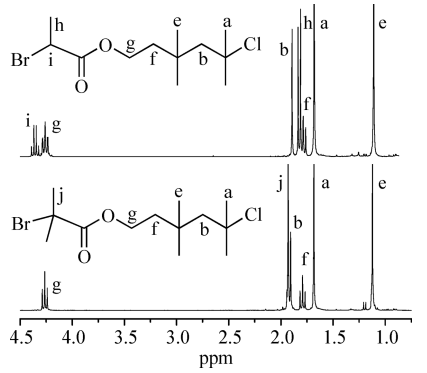

Figure 2. ^{1}H NMR spectra of IB_2BP (upper) and IB_2BMP (lower).

Table 1. Effect of $[TiCl_4]_0$ on IB_2BMP-Initiated Polymerizations[a]

			NMR			GPC			
run	$[TiCl_4]_0/[I]_0$	time[b] (min)	$X_{n,PIB}$	$X_{n,theo}$	I_{eff}	$M_{n,PIB}$ (g/mol)	$M_{n,theo}$ (g/mol)	I_{eff}	PDI
1	3	370	102	82	0.80	6750	4900	0.73	1.08
2	4	120	128	82	0.64	8410	4900	0.58	1.05
3	5	110	118	82	0.70	7680	4900	0.64	1.11
4	6	40	123	82	0.67	7570	4900	0.65	1.11
5	7	35	120	82	0.68	7300	4900	0.67	1.09

[a] 60/40 Hex/MeCl cosolvents (v/v); −70 °C; $[IB]_0$ = 1.00 M; $[IB_2BMP]_0$ = 12.2 mM; $[2,6\text{-lutidine}]_0$ = 4.00 mM. [b] Time required to reach 6 half-lives for monomer consumption (98.4% IB conversion).

group shifted downfield to 4.2 ppm (peak g). In addition, a new doublet at 1.8 ppm (peak h) and a quartet at 4.3 ppm (peak i) appeared for the methyl and methine protons in the newly incorporated 2-bromopropionoyl group, as shown in the upper spectrum. Likewise, a singlet at 1.9 ppm (peak j) appeared for the methyl protons in the 2-bromo-2-methylpropionoyl group, as shown in the lower spectrum. For both spectra, the integrated peak areas were in excellent agreement with the theoretical values.

The last step of the synthesis was substitution of the tertiary hydroxyl group by chlorine for both intermediates. As this reaction increased deshielding of adjacent methyl and methylene protons in both products, their proton NMR peaks shifted downfield to 1.6 ppm (peak a) and 1.9 ppm (peak b), as shown in Figure 2.

PIB Synthesis. Various PIBs with α-bromoester head groups were prepared from both initiators via QCP (Tables 1−4). Figure 3 shows ^{1}H NMR spectra of representative PIBs

Table 2. Effect of Temperature on IB_2BMP-Initiated Polymerizations[a]

			NMR			GPC			
run	temp (°C)	time[b] (min)	$X_{n,PIB}$	$X_{n,theo}$	I_{eff}	$M_{n,PIB}$ (g/mol)	$M_{n,theo}$ (g/mol)	I_{eff}	PDI
4	−70	40	123	82	0.67	7570	4900	0.65	1.11
6	−60	85	107	82	0.77	7230	4900	0.68	1.10
7	−50	170	91	82	0.90	5610	4900	0.81	1.15

[a] 60/40 Hex/MeCl cosolvents (v/v); $[IB]_0$ = 1.00 M; $[IB_2BMP]_0$ = 12.2 mM; $[TiCl_4]_0$ = 73.2 mM; $[2,6\text{-lutidine}]_0$ = 4.00 mM. [b] Time required to reach 6 half-lives for monomer consumption (98.4% IB conversion).

Table 3. Effect of Solvent Polarity on IB_2BMP-Initiated Polymerizations[a]

			NMR			GPC			
run	Hex/MeCl (v/v)	time[b] (min)	$X_{n,PIB}$	$X_{n,theo}$	I_{eff}	$M_{n,PIB}$ (g/mol)	$M_{n,theo}$ (g/mol)	I_{eff}	PDI
2	60/40	120	128	82	0.64	8410	4900	0.58	1.05
8	50/50	50	119	82	0.69	8060	4900	0.61	1.07
9	20/80	10	121	82	0.68	7770	4900	0.63	1.15

[a] At −70 °C; $[IB]_0$ = 1.00 M; $[IB_2BMP]_0$ = 12.2 mM; $[TiCl_4]_0$ = 48.8 mM; $[2,6\text{-lutidine}]_0$ = 4.00 mM. [b] Time required to reach 6 half-lives for monomer consumption (98.4% IB conversion).

initiated by IB_2BP (upper) and IB_2BMP (lower). Large peaks for the methyl and methylene protons in the isobutylene repeat units were observed at 1.1 ppm (peak c) and 1.4 ppm (peak d), respectively. Peaks due to the methyl groups within the α-bromoacyl groups at 1.82 ppm (doublet, h, IB_2BP) and 1.93 ppm (singlet, j, IB_2BMP) and the triplet due to the methylene protons next to the ester linkage at about 4.2 ppm (peak g) were present in both spectra, indicating that the α-bromoester head groups survived intact during QCP. For both polymers, as determined by integration of peak g relative to the combined peaks characteristic of the tail group of the polymer[31] (*tert*-Cl plus possible fractions of *exo*- and *endo*-olefin[32]), the number of α-bromoester head groups was approximately equal to the number of total polymer chains, indicating that protic initiation and transfer to monomer were absent and all chains contained the desired ATRP initiating sites.

To optimize polymerization conditions for QCP of IB, parameters that control the active chain end concentration, including the initial concentration of $TiCl_4$ catalyst ($[TiCl_4]_0$), polymerization temperature, polarity of cosolvent mixture, and targeted number-average molecular weight ($\bar{M}_{n,theo}$) were examined systematically for both initiators.

The influence of $TiCl_4$ concentration was first investigated (Table 1). QCPs of IB (1.0 M) were performed at −70 °C using IB_2BMP as the initiator, 2,6-lutidine as Lewis base in 60/40 (v/v) Hex/MeCl cosolvents, targeting $\bar{M}_{n,theo}$ = 4900 g/mol. Polymerization time listed in the tables is the observed time to reach 6 half-lives (98.4% IB conversion) as determined from ReactIR data; the actual time from catalyst addition to reaction termination was typically between 6.2 and 9 half-lives. As shown in eq 2, the number-average degree of polymerization ($\bar{X}_{n,PIB}$) was determined by ^{1}H NMR spectroscopy using the ratio of the integrated peak area, A_{Me}, of the methyl protons in the isobutylene repeat unit (peak c, 1.1 ppm) to that of the sum of all chain ends, A_{CE}, which was calculated as eq 3 and includes the methylene protons of *tert*-Cl (peak b, 1.96 ppm) chain ends and olefinic protons of possible *exo*-olefin (4.63 ppm), *endo*-olefin (5.15 ppm), and coupled (4.82 ppm) chain ends. Number-average

Table 4. Effect of $[IB_2BMP]_0$ on Polymerization at Several Temperatures[a]

				NMR			GPC			
run	$[IB_2BMP]_0$ (mmol/L)	temp (°C)	time[b] (min)	$X_{n,PIB}$	$X_{n,theo}$	I_{eff}	$M_{n,PIB}$ (g/mol)	$M_{n,theo}$ (g/mol)	I_{eff}	PDI
10	20.8	−70	70	94	48	0.51	5630	3000	0.53	1.10
2	12.2	−70	120	128	82	0.64	8410	4900	0.58	1.05
11	6.1	−70	160	201	164	0.82	11370	9500	0.84	1.06
12	12.2	−60	290	107	82	0.77	7070	4900	0.69	1.06
13	6.1	−60	450	200	164	0.82	11060	9500	0.86	1.10
7[c]	12.2	−50	170	91	82	0.90	5610	4900	0.87	1.15
14[d]	6.1	−50	320	201	164	0.82	10880	9500	0.87	1.09

[a] 60/40 Hex/MeCl cosolvents (v/v); $[IB]_0 = 1.00$ M; $[TiCl_4]_0 = 48.8$ mM; $[2,6\text{-lutidine}]_0 = 4.00$ mM. [b] Time required to reach 6 half-lives for monomer consumption (98.4% IB conversion). [c] $[TiCl_4]_0 = 62.5$ mM. [d] $[TiCl_4]_0 = 73.2$ mM.

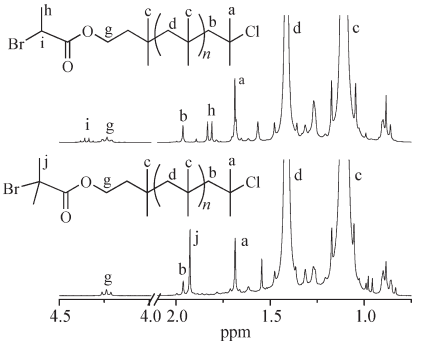

Figure 3. ^{1}H NMR spectra of BP-PIB (run 15, upper) and BMP-PIB (run 2, lower).

molecular weight ($\bar{M}_{n,PIB}$) and polydispersity index (PDI) were determined by GPC/MALLS using the known dn/dc method. I_{eff} was calculated as $\bar{X}_{n,theo}/\bar{X}_{n,PIB}$ and $\bar{M}_{n,theo}/\bar{M}_{n,PIB}$ from NMR and GPC/MALLS data, respectively. As shown in Table 1, I_{eff}'s determined by the two methods were in fair agreement and low relative to a single-cationic-site initiator such as 2-chloro-2-methyl-2,4,4-trimethylpentane (TMPCl).

$$\bar{X}_{n,PIB} = \frac{A_{Me}/6}{A_{CE}} - 1 \qquad (2)$$

$$A_{CE} = A_{exo} + A_{endo} + A_{tert\text{-}Cl}/6 + 2A_{coupled} \qquad (3)$$

For the five runs in Table 1, PDIs were narrow (≤1.15). As $[TiCl_4]_0$ was raised from 36.6 to 85.4 mM, the polymerization time decreased from over 6 h to about 0.5 h. This increase in polymerization rate reflects a progressive shift in the ionization equilibrium toward a higher concentration of active propagating species, controlled by the effective equilibrium constant, $K_{eq}[TiCl_4]^2$. However, I_{eff} was consistently < 1 and did not change significantly with increasing $[TiCl_4]_0$. Faust et al.[33] reported $I_{eff} < 1$ for the related initiator, 5-chloro-3,3,5-trimethylhexyl methacrylate, which also contains an ester group, and these authors suggested that complexation of $TiCl_4$ with the carbonyl group was the likely cause of low I_{eff}. Breland, Murphy, and Storey[27] observed low initiation efficiency with the acetate ester of this compound and likewise attributed low I_{eff} to complexation with the Lewis acid. However, if complexation were the cause, one would reasonably expect initiation efficiency to steadily diminish with increasing $[TiCl_4]_0$. However, initiation efficiency was insensitive to $[TiCl_4]_0$ based on the data in Table 1, and this suggests that complexation is not the reason, or least not the principal reason, for low initiation efficiency.

ReactIR provided a means to monitor real-time [IB] during the polymerization. Figure 4 compares $\ln([M]_0/[M])$ vs polymerization time plots for polymerizations initiated by IB_2BMP and TMPCl, at the same reaction conditions. Polymerization initiated by IB_2BMP was slower, and the first-order plot showed upward curvature, indicating the overall polymerization rate increased as reaction continued. This behavior is consistent with slow initiation for IB_2BMP-initiated polymerizations. In fact, initiation was not only slow; it was incomplete at this monomer/initiator ratio, as supported by the detection of unreacted IB_2BMP in the MeOH wash. Slow initiation by IB_2BMP produced an asymmetric peak in the GPC trace, with a characteristic low molecular weight tail, as shown in Figure 5.

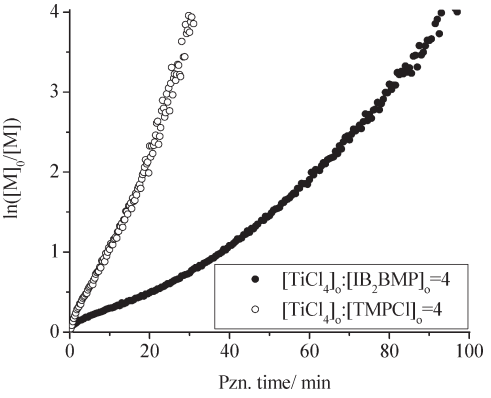

Figure 4. First-order kinetic plots for IB polymerizations initiated by IB_2BMP (Table 1, Run 2) and TMPCl. 60/40 Hex/MeCl cosolvents (v/v); −70 °C; $[IB]_0 = 1.00$ M; $[I]_0 = 12.2$ mM; $[TiCl_4]_0 = 48.8$ mM; $[2,6\text{-lutidine}]_0 = 4.00$ mM.

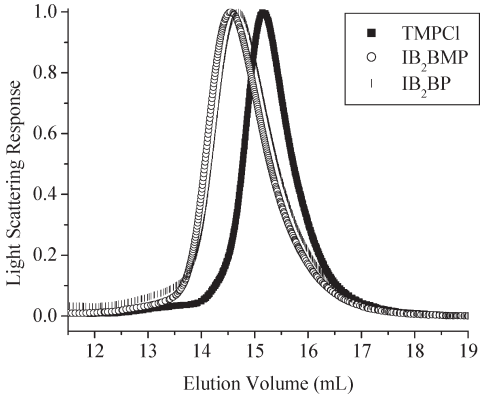

Figure 5. GPC elution curves for IB polymerizations initiated by TMPCl, IB_2BMP (Table 1, Run 2), and IB_2BP (Table 5, Run 16). 60/40 Hex/MeCl cosolvents (v/v); −70 °C; $[IB]_0 = 1.00$ M; $[I]_0 = 12.2$ mM; $[TiCl_4]_0 = 48.8$ mM; $[2,6\text{-lutidine}]_0 = 4.00$ mM. For the TMPCl-initiated control sample: $X_{n,PIB}$ (NMR) = 87; I_{eff} (NMR) = 0.94; $M_{n,PIB}$ (GPC) = 4920 g/mol; PDI (GPC) = 1.01; I_{eff} (GPC) = 0.97.

Table 5. Effect of $[IB_2BP]_0$ on IB Polymerization[a]

			NMR			GPC			
run	$[IB_2BP]_0$ (mmol/L)	time[b] (min)	$X_{n,PIB}$	$X_{n,theo}$	I_{eff}	$M_{n,PIB}$ (g/mol)	$M_{n,theo}$ (g/mol)	I_{eff}	PDI
15[c]	20.8	35	82	48	0.59	5160	3000	0.58	1.06
16	12.2	110	117	82	0.70	7590	4900	0.65	1.12
17	6.1	250	183	164	0.90	11 460	9500	0.83	1.10

[a] 60/40 Hex/MeCl cosolvents (v/v); −70 °C; $[IB]_0$ = 1.00 M; $[TiCl_4]_0$ = 48.8 mM; $[2,6\text{-lutidine}]_0$ = 4.00 mM. [b] Time required to reach 6 half-lives for monomer consumption (98.4% IB conversion). [c] $[TiCl_4]_0$ = 62.5 mM.

Table 6. ATRP[a] of Methyl Acrylate Initiated from PIB Macroinitiators[b]

	NMR		GPC		
run	$X_{n,PMA}$	wt % PMA	$M_{n,PMA}$ (g/mol)	PDI	wt % PMA
BP-PIB-*b*-PMA_{60}	68	52.4	5780	1.06	50.9
BP-PIB-*b*-PMA_{90}	80	56.5	7020	1.04	55.8
BP-PIB-*b*-PMA_{120}	112	64.5	12900	1.14	69.8
BMP-PIB-*b*-PMA_{60}	62	53.5	6020	1.04	56.4
BMP-PIB-*b*-PMA_{90}	90	62.5	8970	1.04	65.9
BMP-PIB-*b*-PMA_{120}	126	70.0	13760	1.05	74.7

[a] $[MacroI]_0:[CuBr]_0:[PMDETA]_0$ = 1:1:1 ($[MacroI]_0$ = 0.05 M) in toluene at 70 °C; 0.60$[MA]_0/[MacroI]_0$ = 60, 90, or 120. [b] BP-PIB: M_n = 5570 g/mol and PDI = 1.04 (GPC); X_n = 89 by NMR. BMP-PIB: M_n = 4650 g/mol and PDI = 1.02 (GPC); X_n = 77 by NMR.

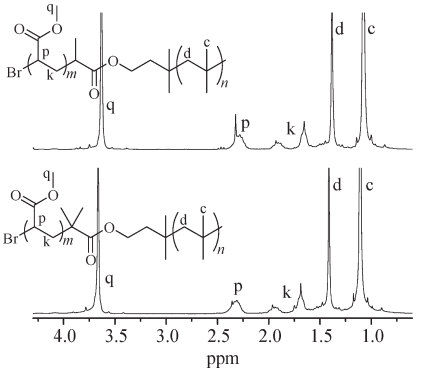

Figure 6. ^1H NMR spectra of of BP-PIB-*b*-PMA_{60} (upper) and BMP-PIB-*b*-PMA_{60} (lower).

As $[TiCl_4]_0$ did not influence I_{eff} significantly, the value of $[TiCl_4]_0$ was chosen to complete polymerizations within a reasonable amount of time for all the experiments discussed below.

The influence of polymerization temperature on I_{eff} was next investigated over the range −70 to −50 °C, employing IB_2BMP as the initiator. Polymerization conditions and results are listed in Table 2. In general, polymerization rate decreased with increasing temperature, consistent with the well-known negative apparent activation energy for IB polymerization under these conditions.[34] At the same time, number-average molecular weight, characterized by GPC, decreased from 155% to 114% of theoretical. This clearly shows that I_{eff} increases with increasing polymerization temperature, which is consistent with the fact that the apparent activation energy for ionization by $TiCl_4$ is greater than that for propagation; i.e., run number decreases with increasing temperature.[35]

The influence of solvent polarity was next investigated at −70 °C, employing IB_2BMP as the initiator. These experiments were conducted in part to eliminate the possibility that low I_{eff} resulted from incompletely dissolved initiator. Polymerization conditions and results are listed in Table 3. Reaction time decreased from 2 h to about 10 min as the volume percentage of MeCl in the cosolvents was increased from 40 to 80. However, I_{eff} was essentially unchanged with increasing medium polarity, which confirmed that initiator solubility is not the cause of low I_{eff}.

The effect of IB_2BMP initiator concentration (at constant [IB] = 1 M) was investigated at several temperatures, targeting $\bar{M}_n$s of 3000 g/mol (3K), 5000 g/mol (5K), and 10 000 g/mol (10K). Polymerization conditions and results are listed in Table 4. Different $[TiCl_4]_0$ were applied to adjust the polymerization time. At −70 °C, as the targeted $\bar{M}_n$ was increased from 3K, 5K, to 10K, I_{eff} (GPC) increased from 53%, 58%, to 83%, as expected. The same trend was observed for the polymerizations performed at −60 °C, consistent with slow initiation. At −50 °C, the I_{eff} for 5K and 10K were about same, ∼87%.

All polymerizations discussed above were initiated by IB_2BMP. Polymerizations of IB were also performed using IB_2BP as the initiator, targeting $\bar{M}_n$s of 3K, 5K, and 10K. Polymerization conditions and results are listed in Table 5. Different $[TiCl_4]_0$ were used to adjust the polymerization time. At −70 °C, as the targeted $\bar{M}_n$ was raised from 3K, 5K, to 10K, I_{eff} (GPC) increased from 58%, 65%, to 83%, revealing the same tendency as IB_2BMP. GPC elution curves (see representative curve in Figure 5) showed low molecular weight tailing, indicating slow initiation. In general, under the same conditions, IB_2BP produced slightly higher I_{eff} compared to IB_2BMP.

PIB-*b*-PMA Synthesis. ATRP was demonstrated from both α-bromoester-functionalized PIB macroinitiators (BP-PIB and BMP-PIB) using methyl acrylate (Table 6). Polymerizations were monitored and terminated at 60% conversion in order to avoid termination or chain transfer reactions. Figure 6 shows ^1H NMR spectra of BP-PIB-*b*-PMA_{60} (upper) and BMP-PIB-*b*-PMA_{60} (lower), which are representative. Peaks due to the PMA block appeared at 3.6 (peak k), 2.3 (peak j), and 1.4−2.0 ppm (peak i). Tacticy effects caused the PMA methylene protons to exist in three different chemical environments and thus exhibit three major peaks in the range 1.4−2.0 ppm.[36]

Compositions of block copolymers listed in Table 6 were calculated from both ^1H NMR spectroscopy and GPC, considering the IB_2BMP or IB_2BP residue as part of the PIB block. $\bar{X}_{n,PMA}$ was calculated from the ratio of the integrated peak area of the methyl hydrogens of the PMA block, $A_{3.6\,ppm}$, to that of the *gem*-dimethyl hydrogens of the PIB block, $A_{1.1\,ppm}$, via eq 4. Weight percentage of PMA in the block copolymer was calculated using eq 5, where M_{IB}, M_{MA}, and M_I are the molecular weights for IB, methyl acrylate, and the initiator, respectively. $\bar{M}_{n,PIB\text{-}b\text{-}PMA}$ and PDI of block copolymers were obtained by GPC-MALLS using two mixed D columns and a d*n*/d*c* calculated from the refractive index detector response and assuming 100% mass recovery from the columns. Number-average molecular weight of the PMA block, $\bar{M}_{n,PMA}$, and copolymer composition were calculated from GPC data using eqs 6 and 7, respectively. PIB-*b*-PMA diblock copolymer

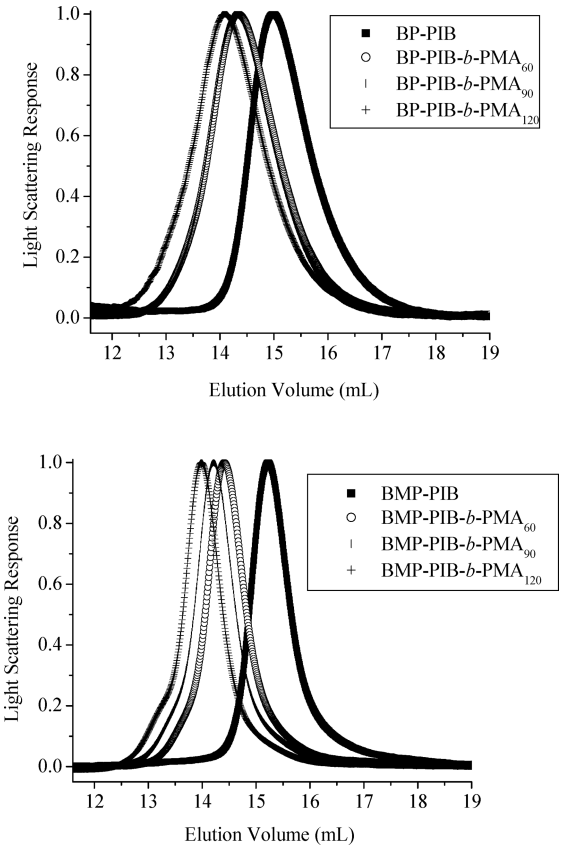

Figure 7. GPC elution curves (crude samples prior to precipitation) of BP-PIB-*b*-PMA (upper) and BMP-PIB-*b*-PMA (lower) with different length of PMA block.

compositions characterized by these two methods were comparable.

$$\bar{X}_{\mathrm{n,PMA}}\ (\mathrm{NMR}) = \frac{A_{3.6\mathrm{ppm}}}{A_{1.1\mathrm{ppm}}/2}(\bar{X}_{\mathrm{n,PIB}} + 1) \qquad (4)$$

$$\mathrm{wt\ \%\ PMA\ (NMR)} = \frac{\bar{X}_{\mathrm{n,\,PMA}} M_{\mathrm{MA}}}{\bar{X}_{\mathrm{n,\,PIB}} M_{\mathrm{IB}} + \bar{X}_{\mathrm{n,\,PMA}} M_{\mathrm{MA}} + M_{\mathrm{I}}} \times 100\% \qquad (5)$$

$$\bar{M}_{\mathrm{n,PMA}}\ (\mathrm{GPC}) = \bar{M}_{\mathrm{n,PMA\text{-}}b\text{-}\mathrm{PIB}} - \bar{M}_{\mathrm{n,PIB}} \qquad (6)$$

$$\mathrm{wt\ \%\ PMA\ (GPC)} = \frac{\bar{M}_{\mathrm{n,PMA}}}{\bar{M}_{\mathrm{n,PIB\text{-}}b\text{-}\mathrm{PMA}}} \times 100\% \qquad (7)$$

GPC characterization (Figure 7) showed that low PDI diblock polymers were obtained and that no unreacted MacroI was present. This indicated that the α-bromoester functional groups of both IB_2BP and IB_2BMP remained intact during QCP and that ATRP initiation was quantitative. As the target degree of polymerization of the PMA block increased, GPC elution peaks shifted to the left, as expected. However, for systems targeting the highest PMA degree of polymerization, radical−radical coupling occurred, as evidenced by a high molecular weight shoulder in the GPC curve (see BMP-PIB-*b*-PMA_{120} in Figure 7).

Conclusion

New dual initiators, IB_2BMP and IB_2BP, containing both a cationic polymerization initiating site and an ATRP initiating site, were designed for the preparation of PIB-based AB diblock and ABC triblock copolymers. Both initiators were successfully synthesized in four steps, as confirmed by ^{1}H NMR spectroscopy. When used for the QCP of IB, low initiation efficiencies (I_{eff}), caused by slow initiation, were observed for both initiators. To optimize the conditions for QCP and to examine the cause for low I_{eff}, polymerization conditions including the initial concentration of catalyst ($[TiCl_4]_0$), temperature, solvent polarity, and targeted number-average molecular weight ($\bar{M}_{\mathrm{n}}$) were examined. The observed I_{eff} for all reactions were less than 1 for both initiators within the range of conditions examined. However, increasing polymerization temperature significantly improved I_{eff}, and at −50 °C, about 90% efficiency was achieved for IB_2BMP at a target molecular weight of 5K, i.e., for $[IB]_0/[IB_2BMP]_0 = 82$. As expected, I_{eff} increased with increasing target molecular weight. Changes in $[TiCl_4]$ and solvent polarity caused negligible changes in I_{eff}. Complexation between $TiCl_4$ and the carbonyl oxygen of 3,3,5-trimethyl-5-chlorohexyl esters has been proposed[27,32] as a reason for low I_{eff}, but this seems inconsistent with the absence of any correlation between I_{eff} and $[TiCl_4]$.

Further investigations directed to the origin and solution of low I_{eff} are ongoing and will be reported in a subsequent paper. However, the following points can be presently made for optimal use of either initiator. If the initiator is being used to create low molecular weight PIB, then a relatively high polymerization temperature, e.g., −60 to −50 °C, is advantageous since the lower propagation run number[36] boosts I_{eff} and lowers PDI. If the initiator is being used to create high molecular weight PIB, the high monomer/initiator ratio will ensure $I_{\mathrm{eff}} \cong 1.0$ and low PDI regardless of temperature, and therefore a lower temperature such as −80 °C is preferred to maximize livingness.

PIBs with 2-bromo-2-methylpropionate (BMP-PIB) or 2-bromopropionate (BP-PIB) head groups were successfully used for ATRP of MA. Targeted $\bar{M}_{\mathrm{n}}$ and narrow PDIs were obtained for both macroinitiators. No macroinitiator residue was observed via GPC, indicating that the α-bromoester functional groups remained intact during QCP.

References and Notes

(1) Kaszas, G.; Puskas, J. E.; Kennedy, J. P.; Hager, W. G. *J. Polym. Sci., Part A: Polym. Chem. Ed.* **1991**, *29*, 421–426.
(2) Kaszas, G.; Puskas, J. E.; Kennedy, J. P.; Hager, W. G. *J. Polym. Sci., Polym. Chem. Ed.* **1991**, *29*, 427–435.
(3) Tsunogae, Y.; Kennedy, J. P. *J. Polym. Sci., Part A: Polym. Chem. Ed.* **1994**, *32*, 403–412.
(4) Li, D.; Faust, R. *Macromolecules* **1995**, *28*, 1383–1389.
(5) Kwon, Y.; Cao, X.; Faust, R. *Macromolecules* **1999**, *32*, 6963–6968.
(6) Puskas, J. E.; Kaszas, G.; Kennedy, J. P.; Hager, W. G. *J. Polym. Sci., Part A: Polym. Chem. Ed.* **1992**, *30*, 41–48.
(7) Fodor, Z.; Faust, R. *J. Macromol. Sci., Part A: Pure Appl. Chem.* **1994**, *A31*, 1985–2000.
(8) Kennedy, J. P.; Kurian, J. *J. Polym. Sci., Part A: Polym. Chem.* **1990**, 3725–3738.
(9) Hadjikyriacou, S.; Faust, R. *Macromolecules* **1996**, *29*, 5261–5267.
(10) Matyjaszewski, K. *Macromol. Symp.* **1998**, *132*, 85–101.
(11) Zheng, F.; Kennedy, J. P. *J. Polym. Sci., Part A: Polym. Chem.* **2002**, *40*, 3662–3678.
(12) Storey, R. F.; Scheuer, A. D.; Achord, B. C. *Polymer* **2005**, *46*, 2141–2152.
(13) Storey, R. F.; Scheuer, A. D.; Achord, B. C. *J. Macromol. Sci., Part A: Pure Appl. Chem.* **2006**, *43*, 1493–1512.
(14) Coca, S.; Matyjaszewski, K. *Macromolecules* **1997**, *30*, 2808–2810.
(15) Jakubowski, W.; Tsarevsky, N. V.; Higashihara, T.; Faust, R.; Matyjaszewski, K. *Macromolecules* **2008**, *41*, 2318–2323.
(16) Magenau, A. J. D.; Martinez-Castro, N.; Savin, D. A.; Storey, R. F. *Macromolecules* **2009**, *42*, 2353–2359.

(17) Magenau, A. J. D.; Martinez-Castro, N.; Storey, R. F. *Macromolecules* **2009**, *42*, 8044–8051.
(18) Feng, D.; Chandekar, A.; Whitten, J. E.; Faust, R. *ACS Div. Polym. Chem., Polym. Prepr.* **2007**, *48* (2), 1017–1018.
(19) Martinez-Castro, N.; Zhang, M.; Pergushov, D. V.; Mueller, A. H. E. *Des. Monomers Polym.* **2006**, *9*, 63–79.
(20) Martinez-Castro, N.; Lanzendoerfer, M. G.; Mueller, A. H. E.; Cho, J. C.; Acar, M. H.; Faust, R. *Macromolecules* **2003**, *36*, 6985–6994.
(21) Kwon, Y.; Faust, R. *J. Macromol. Sci., Part A: Pure Appl. Chem.* **2005**, *A42*, 385–401.
(22) Kwon, Y.; Faust, R.; Chen, C. X.; Thomas, E. L. *Macromolecules* **2002**, *35*, 3348–3357.
(23) Bernaerts, K. V.; Du Prez, F. E. *Polymer* **2005**, *46*, 8469–8482.
(24) Bernaerts, K. V.; Schacht, E. H.; Goethals, E. J.; Du Prez, F. E. *J. Polym. Sci., Part A: Polym. Chem.* **2003**, *41*, 3206–3217.
(25) Bernaerts, K. V.; Willet, N.; Van Camp, W.; Jérôme, R.; Du Prez, F. E. *Macromolecules* **2006**, *39*, 3760–3769.
(26) Becer, C. R.; Paulus, R. M.; Hoppener, S.; Hoogenboom, R.; Fustin, C.-A.; Gohy, J.-F.; Schubert, U. S. *Macromolecules* **2008**, *41*, 5210–5215.
(27) Breland, L. K.; Murphy, J. C.; Storey, R. F. *Polymer* **2006**, *47*, 1852–1860.
(28) Chance, R. R.; Baniukiewicz, S. P.; Mintz, D.; Ver Strate, G.; Hadjichristidis, N. *Int. J. Polym. Anal. Charact.* **1995**, *1* (1), 3–34.
(29) Storey, R. F.; Donnalley, A. B.; Maggio, T. L. *Macromolecules* **1998**, *31*, 1523–1526.
(30) Iovu, M. C.; Jeffries-EL, M.; Sheina, E. E.; Cooper, J. R.; McCullough, R. D. *Polymer* **2005**, *46*, 8582–8586.
(31) Simison, K. L.; Stokes, C. D.; Harrison, J. J.; Storey, R. F. *Macromolecules* **2006**, *39*, 2481–2487.
(32) It is common to observe olefinic end groups in $TiCl_4$-coinitiated isobutylene polymerizations at higher temperatures such as those reported here, e.g., −50 °C. These structures result from unimolecular proton transfer to the paired counterion. This process does not cause loss of control over molecular weight, nor does it create any chains without the desired ATRP initiating sites because the eliminated proton cannot initiate a new chain in the presence of proton traps and/or strong bases such as 2,6-lutidine. These concepts are discussed in detail in the following paper: Fodor, Zs.; Bae, Y. C.; Faust, R. *Macromolecules* **1998**, *31*, 4439–4446.
(33) Balogh, L.; Takacs, A.; Faust, R. *ACS Div. Polym. Chem., Polym. Prepr.* **1992**, *33* (1), 958–959.
(34) Storey, R. F.; Choate, K. R., Jr. *Macromolecules* **1997**, *30*, 4799–4806.
(35) Smith, Q. A.; Storey, R. F. *Macromolecules* **2005**, *38*, 4983–4988.
(36) Brar, A. S.; Goyal, A. K.; Hooda, S. *J. Mol. Struct.* **2008**, *885*, 15–17.